Preparation and electrochemical properties of nanoparticle structural LiFePO$_4$/C by Sol–Gel method as cathode material for lithium ion batteries

Zongfeng Li[1] · **Guixia Dong**[1] · **Jingrui Kang**[1] · **Lei Li**[1]

Abstract

In this study, LiFePO$_4$/C nanocomposites with higher capacity and cycle performance are synthesized by sol–gel method using FeCl$_2$·4H$_2$O, H$_3$PO$_4$, Li$_2$CO$_3$, and Citric acid as the starting materials. LiFePO$_4$/C cathode materials with different grain size and electrochemical properties were obtained by changing the calcination temperature of LiFePO$_4$/C precursor prepared by sol–gel method. Specially, the LiFePO$_4$/C precursor prepared by sol–gel method was heated to 700 °C for 12 h under nitrogen atmosphere, and the nanoparticle structural LiFePO$_4$/C was obtained. The first discharge specific capacity is 156.5 mAh g^{-1} at a charging current of 0.2 C. The first discharge specific capacity is 124.5 mAh g^{-1} at a charging current of 1 C, and after the 250th cycles, the discharge specific capacity is 120.7 mAh g^{-1}, the retention rate of discharge specific capacity is 96.9%.

1 Introduction

In the history of secondary batteries, compared with lead–acid batteries [1], nickel–cadmium batteries [2], and nickel–hydrogen batteries [3, 4], lithium-ion batteries have many excellent characteristics, such as high working voltage (3–4 V), high energy density, long cycle life, low self-discharge rate, low pollution and no memory effect [5]. Therefore, lithium-ion batteries have become the research and application hotspot of secondary batteries in the world today. Due to the rapid development of lithium-ion batteries, lithium resources are also facing enormous challenges. Scholars have discovered sodium-ion batteries with huge resources [6]. However, compared with sodium ion batteries, lithium-ion batteries have great advantages in terms of energy density, cycle life and environmental pollution [5].

Since 1997, researchers have discovered that Li$^+$ can be removed and embedded in LiFePO$_4$, and LiFePO$_4$ has the characteristics of low raw material cost, no pollution to the environment, and stable safety performance, which makes LiFePO$_4$ a research hotspot of lithium-ion batteries [7]. LFP (LiFePO$_4$) has a theoretical capacity of 170 mAh g^{-1} and a high voltage platform of about 3.45 V [8]. After years of hard work, LiFePO$_4$ materials have been rapidly applied. Due to the nature of its own structure, LiFePO$_4$ has the disadvantages of very low diffusion rate of ions and poor conductivity, which hinders the further development of LiFePO4 materials [9–11]. At present, researchers mainly adopt three methods of ion doping [12–14], surface of coating material [15] and particle size reduction [16] to improve the conductivity and diffusion rate of materials [17–19].

In 2001, Velence proposed a method to solve the low electrical conductivity of LiFePO$_4$, namely carbon coating and carbothermal reduction technology [20]. after that, the A123SYSTEMS technical team discovered ion doping and nanotechnology that can improve the conductivity of LiFePO$_4$, so LiFePO$_4$ material entered the industrialization stage. In 2009, LiFePO$_4$ was designated as a key research project by China's national high-tech research and development plan new material technology research field, which is China's "863" Plan, "973" Plan and "十一五" Plan [21, 22]. The areas supported by high-tech development planning. At present, LiFePO$_4$ material has become the most

✉ Guixia Dong
    Dongguixia199@163.com

    Zongfeng Li
    1243060784@qq.com

1   Laboratory of Environment Functional Materials
    of Tangshan City, Hebei Provincial Key Laboratory
    of Inorganic Nonmetallic Materials, College of Materials
    Science and Engineering, North China University of Science
    and Technology, Tangshan 063210, Hebei, China

popular cathode material for lithium ion batteries, and is widely used in various fields of social life.

Since LFP has defects such as low ionic conductivity and low ion diffusion rate, it is possible to increase the diffusion rate of ions by reducing the size of the product particles. The liquid phase method [23, 24] is easier to carry out than the solid phase method [25, 26], and only a lower synthesis temperature is required. The diffusion of the components in the sol–gel system is in the nanometer range, while the component diffusion in the solid phase reaction is in the micrometer range, so the reaction is easy to proceed and the temperature is low. Therefore, the $LiFePO_4$/C was prepared by the sol–gel method. The second is to improve the electrochemical performance by modifying the cathode material with carbon coating, mainly by adding a conductive agent on the surface of the particles to improve the conductivity between the particles [27, 28]. However, compared with solid phase method, the sol–gel method has many disadvantages, such as long synthesis time, process cumbersome, a large shrinkage of the precursor during drying, poor sinterability of the powder material, and the powder particle size is not easily controlled in the sintering process [29].

In this article, lithium carbonate, phosphoric acid, ferrous chloride and citric acid were used as raw materials to prepare $LiFePO_4$/C positive electrode materials by sol–gel method [16, 30, 31]. The microstructure and electrochemical properties of lithium iron phosphate cathode materials were investigated by calcination temperature, Selecting materials with good electrochemical properties.

2 Experimental

2.1 Sample preparation and characterization

The $LiFePO_4$/C positive electrode material is prepared by preparing a precursor by a sol–gel method and then calcining. $FeCl_2 \cdot 4H_2O$, H_3PO_4 and Li_2CO_3 were used as the main raw materials, and the raw materials were weighed according to a certain molar ratio (Li: Fe: P = 1.3:1:1). The iron source, the lithium source and the phosphorus source compound of the same mass are respectively added to the solvent (the solvent is anhydrous ethanol added with a mass fraction of 12 wt% citric acid) in a certain order, and the mixture is stirred uniformly, and the stirring is stopped after the reaction is completed. The sol was obtained and sealed to allow for conversion to a gel. The gel was transferred to a 60 °C blast oven for 12 h to allow the gel to dry sufficiently. Part of the sample is taken for thermogravimetric and differential thermal analysis to determine the reaction temperature range of the material. After determining the reaction temperature, the sample is transferred into a quartz porcelain boat, and then placed in a tubular atmosphere furnace, and a protective atmosphere N_2

is introduced to prevent the material was oxidized and heated to 350 °C at 3 °C/min, after 6 h of constant temperature, the temperature was raised to 650～750 °C at a rate of 3 °C/min, and the temperature was kept for 12 h (respectively designated as 650 °C-LFP, 675 °C-LFP, 700 °C-LFP, 725 °C-LFP and 750 °C-LFP). The sample was taken out and ground again, and stored in a dry environment.

The X-ray diffraction (XRD, X'Pert PRO MPD, D8, Ultima IV) with the Cu–Ka source as the incident beam ($\lambda = 1.5406$ Å) at a voltage of 40 kV and a current 100 mA was used to characterize the crystal structure of the synthesized samples, and scanning the 2θ range of 10°–90° at an interval of 0.04°.The scanning electron microscopy (SEM, S-4800, Hitachi, Japan) is used as a tool to investigate the surface morphology of synthetic samples.

2.2 Electrode preparation and electrochemical characterization
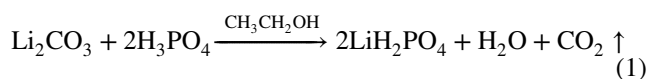
The electrochemical performance of the synthesized samples was investigated using a CR2032 coin cell. In the preparation of the working electrode, the active material, conductive carbon black and polyvinylidene fluoride (PVDF) were mixed at a mass ratio of 8:1:1, and the mixed material that coated onto copper current collectors was dissolved in N-methyl-2-pyrrolidone (NMP) to prepare an electrode. And The electrode disks and cells were prepared in an Ar glovebox. The electrolyte was 1 M LiPF6 in a liquid mixture of ethlylene carbonate (EC), dimethyl carbonate (DMC) and ethyl methyl carbonate (EMC) (volume ratio 1:1:1).
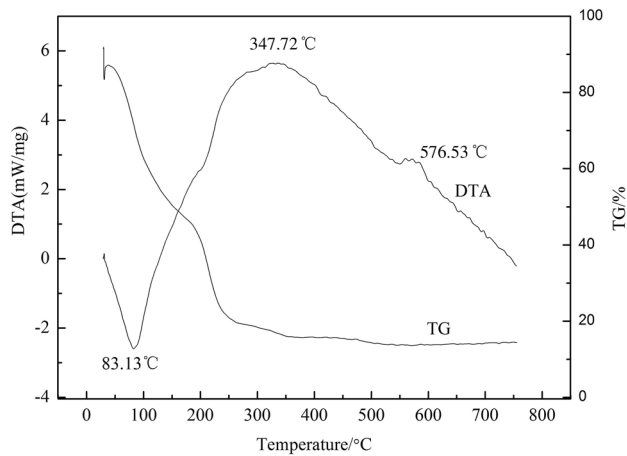
The galvanostatic discharge–charge and cycling performance of $LiFePO_4$/C electrode materials were tested by LAND CT2001A model(Wuhan Jinnuo Electronics Co. Ltd.) at potential window of 2.5–4.2 V. Cyclic voltammetry (CV) was tested by CHI660E B16506 electrochemical workstation from 0.05 to 3.0 V with a sweep speed of 0.1 mV s^{-1}–10 mV s^{-1}. For electrochemical impendence spectroscopy (EIS), its frequencies ranged from 100 kHz–0.01 Hz.

3 Result and discussion

3.1 Phase structure analysis

The TG-DTA of the LiFePO4 precursor prepared by the sol–gel method, the results are showed in Fig. 1. The chemical reaction equation for the synthesis of $LiFePO_4$ powder from inorganic compounds Li_2CO_3, H_3PO_4 and $FeCl_2 \cdot 4H_2O$ is as follows.

$$Li_2CO_3 + 2H_3PO_4 \xrightarrow{CH_3CH_2OH} 2LiH_2PO_4 + H_2O + CO_2 \uparrow \tag{1}$$

$$2FeCl_2 + LiH_2PO_4 \xrightarrow{Ar} 2LiFePO_4 + 2HCl \uparrow \tag{2}$$

Fig. 1 TG-DTA of LiFePO$_4$ precursor prepared by sol–gel method

Fig. 2 XRD patterns of samples at different calcination temperatures

It can be seen from Fig. 1 that when the temperature is at 83.13 °C, the first endothermic peak appears, mainly due to the vaporization of anhydrous ethanol in the dry gel, the weight loss rate is about 15.38%; when the temperature rises to 347.72 °C, the first exothermic peak appeared, mainly due to the chemical reaction of Li$_2$CO$_3$ and H$_3$PO$_4$, and the elimination of crystal water and carbon dioxide gas. The equation is as shown in formula (1), the weight loss rate is about 54.40%; when the temperature continues to rise to 576.53 °C, a second exothermic peak appears on the differential thermal curve, mainly FeCl$_2$ and LiH$_2$PO$_4$ began to participate in the chemical reaction and produced LiFePO$_4$, the chemical reaction equation is shown in formula (2). The weight loss rate at this stage is mainly the volatilization of the reaction product HCl. After 576.25 °C, the TG curve remains basically unchanged, indicating that a pure phase LiFePO4 battery material can be prepared theoretically after 576.25 °C.

Figure 2 shows XRD patterns of 650 °C-LFP, 675 °C-LFP, 700 °C-LFP, 725 °C-LFP and 750 °C-LFP with a carbon loading of 12% by weight. Compared with the standard map JCPDS (83-2092), the samples obtained at different calcination temperatures did form lithium iron phosphate, and the main characteristic diffraction peaks also appeared. The intensity of the diffraction peak of the sample at a calcination temperature of 700 °C is higher than that of other temperatures other temperatures, and the main diffraction peak of 700 °C-LFP is close to the main diffraction peak of the standard spectrum, indicating the crystallinity of the sample at 700 °C better.

3.2 Micromorphology analysis

As shown in Fig. 3, 650 °C-LFP, 675 °C-LFP, 700 °C-LFP, 725 °C-LFP and 750 °C-LFP of the carbon were added in
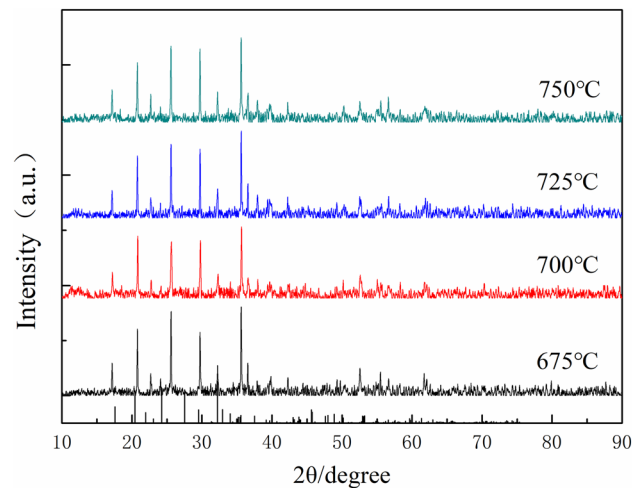
an amount of 12 wt%, theirs' microscopic imaging of the surface of a substance under an electron scanning microscope. It can be seen from Fig. 3 that after the sample is sintered at a high temperature, the shape exhibits a different structure. When the calcination temperature is 700 °C, the particle distribution of the sample is relatively uniform, the particle size is small, and the specific surface area is large, which is favorable for the insertion and extraction of lithium ions. At calcination temperatures of 650 °C and 675 °C, the sample particles were incompletely calcined due to the too low calcination temperature, and the particle size was large and the crystallinity was low. At calcination temperatures of 725 °C and 750 °C, the particle size of the sample sharply increased and the material agglomerated in large amounts because secondary crystallization of the crystal occurred as the calcination temperature increased. Excessive growth of crystal grains and aggregation of material particles lead to an increase in the particle size of the material, which increases the migration distance of lithium ions in the charge and discharge process, thereby reducing the utilization rate of the active material of the material, which not only deteriorates the conductivity but also is not conducive to the insertion and extraction of lithium ions.

In order to prove that the carbon layer was coated on the surface of the crystal, the sample was subjected to energy spectrum test. As shown in Fig. 4, the SEM and EDS dot scan test charts of the LiFePO4/C sample prepared by the carbon addition amount of 12 wt%, the calcination temperature of 700 °C, and the holding time of 12 h. In Fig. 4a, find 3 points to the point on the surface of the particle to make the energy spectrum. As shown in Fig. 4b, the carbon element obtained by the EDS point scan when the energy spectrum is located at the A and C positions. The content is significantly higher than the carbon content at point B, indicating that the carbon layer coated with lithium iron

Fig. 3 SEM image of samples at different calcination temperatures. **a** for 650 °C-LFP, **b** for 675 °C-LFP, **c** for 700 °C-LFP, **d** for 725 °C-LFP, **e** for 750 °C-LFP
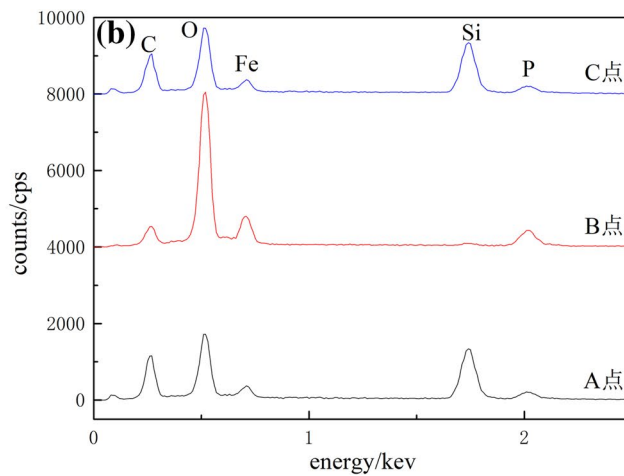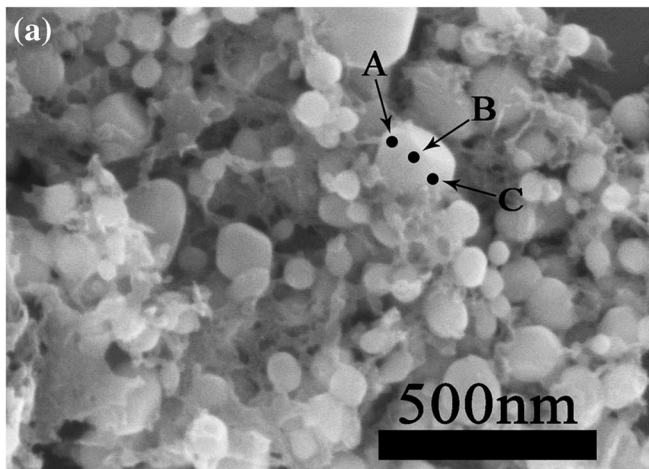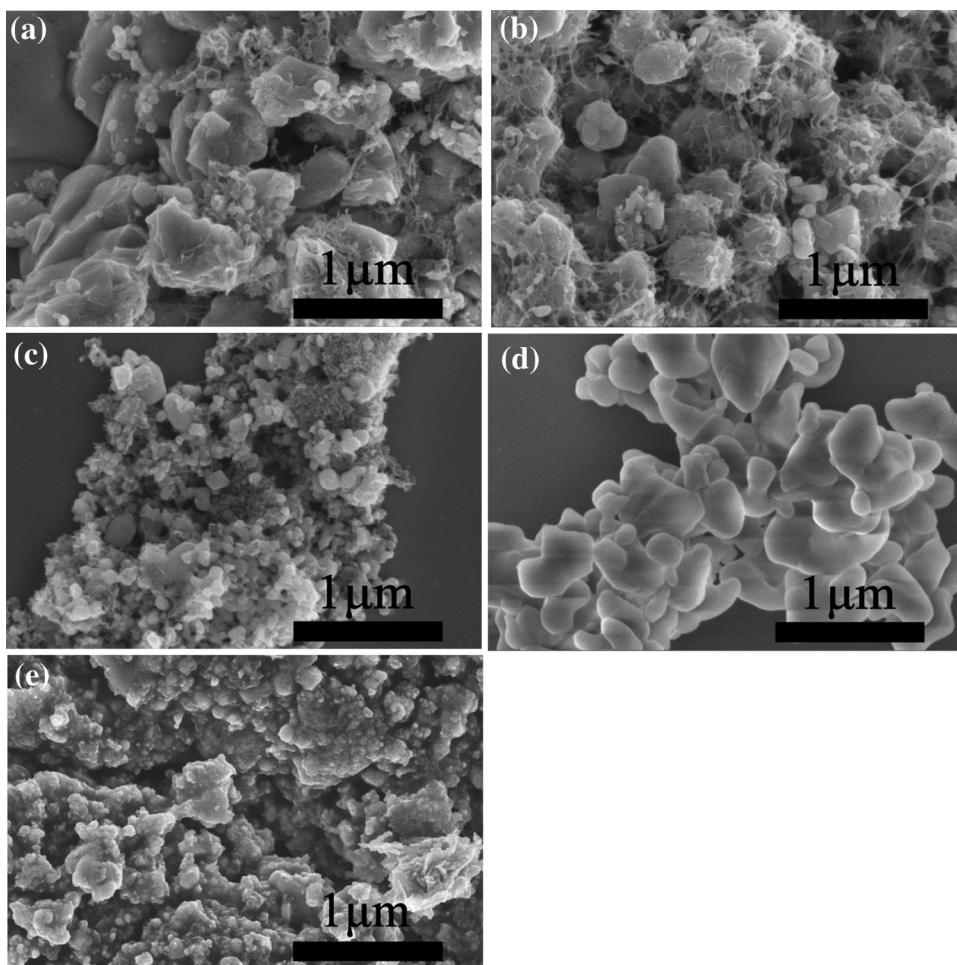
Fig. 4 SEM and EDS diagram of prepared LiFePO$_4$/C sample with calcination temperature of, 700 °C, holding time of 12 h and carbon content of 12 wt%

phosphate is not uniform, but it is proved that the lithium iron phosphate material has indeed completed the carbon coating, in which the points A and C are insufficient due to

the thickness. The X-ray penetrating material impinges on the material carrier silicon wafer to cause the appearance of Si. Since the carbon layer is coated on the outer surface of

the lithium iron phosphate particles, a separator is formed, thereby limiting the agglomeration and secondary growth of the crystal, and is advantageous for improving the electrochemical performance.

### 3.3 Electrochemical analysis

Rate performance is an indispensable part of testing the electrochemical performance of lithium-ion batteries. As shown in Fig. 5a, the batteries prepared by using lithium iron phosphate cathode materials having different calcination temperatures have the rate performance at current densities of 0.2 C, 0.5 C, 1 C, 2 C, 5 C and 10 C, respectively. As can be seen from Fig. 5, when the calcination temperature is 700 °C (700 °C-LFP), the specific capacity of the battery at 0.2 C to 10 C is higher than that of other calcination temperatures. The specific discharge capacities at each magnification were 156.5 mAh g^{-1}, 140.2 mAh g^{-1}, 121.6 mAh g^{-1}, 95.6 mAh g^{-1}, 76.3 mAh g^{-1} and 70.9 mAh g^{-1}, respectively. The discharge specific capacity decreases with the increase of current density, and the discharge specific capacity decline rate is relatively stable at a magnification of 0.5 ~ 10 C. When the calcination temperature is 700 °C (700 °C-LFP), the current density decreases from 10 C to 0.2 C, and the specific discharge capacity is 156.9 mAh g^{-1},

which is slightly higher than the first current density of 0.2 C, it may be that the electrode material is activated as the charge and discharge progress, resulting in a certain increase in battery capacity. By comparing with the results of other scholars, the effectiveness of this experiment is demonstrated, as shown in Table 1.

In order to better understand the degree of attenuation of the discharge specific capacity of LiFePO$_4$/C cathode material, the constant current charge and discharge performance test of the battery prepared for different calcination temperature samples at a current density of 0.2 C is shown in Fig. 6. It can be seen from Fig. 6 that the discharge platforms of different samples all appear around 3.4 V, and the charging platforms are all around 3.5 V, of which 700 °C-LFP has the widest charge and discharge platform, and the discharge specific capacity is up to 156.5 mAh g^{-1}. By observing the curves of 650 °C-LFP and 675 °C-LFP, there are two charging platforms. The voltage of the first charging platform is close to 3.5 V, and the voltage of the second charging platform is close to 4.1 V, it is indicated that when 650 °C-LFP and 675 °C-LFP is charged, lithium ions in the deep layers of the particles are also exchanged, but when discharging, the lithium ions embedded in the deep portions fail to extract, resulting in the reduction in discharge capacity. The results
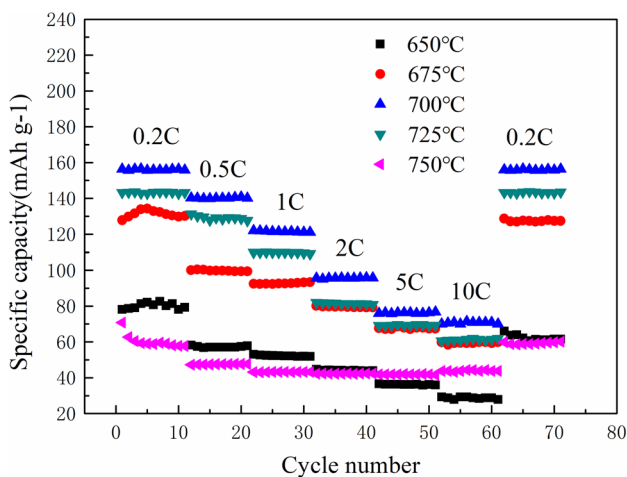
Fig. 5 Specifc charge and discharge capacities at various current rates of samples at different calcination temperatures
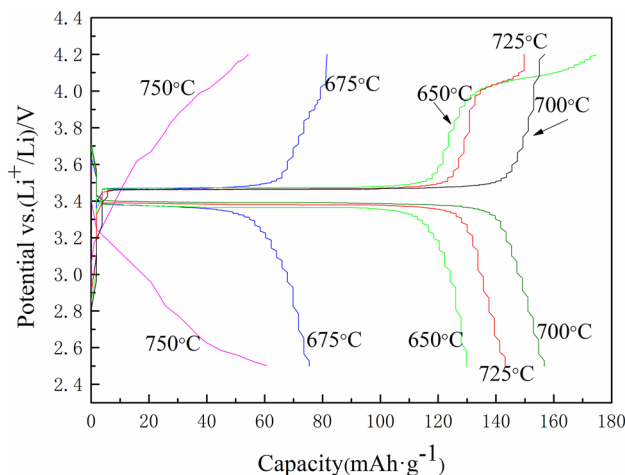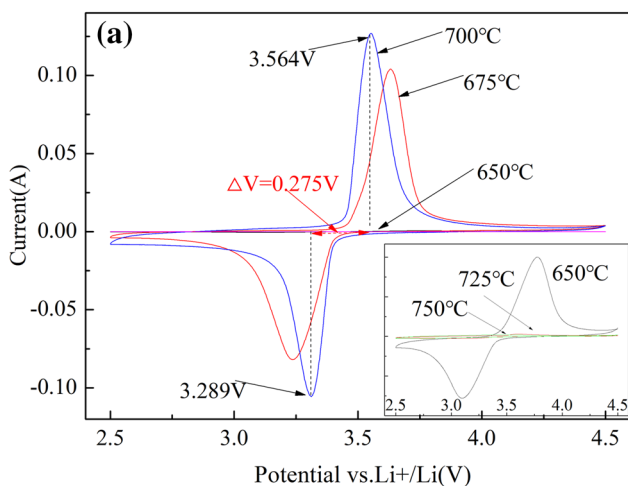

Fig. 6 Electrochemical performance of initial charge–discharge curves at different current rates of samples at different calcination temperatures

Table 1 LFP/C with different electrochemical properties

| Structural formula	Nano-structural	Platform potential (V)	Capacity (mAh g^{-1})	Ref
LiFePO4/C	Particles	3.4	159.3 at 0.1 C	[26]
LiFePO4/C	Meso-porous structure	3.3	166.7 at 0.2 C	[25]
C/LFP/MWCNTs	3D layered pore structure	3.4	169.6 at 0.1 C	[32]
LiFePO4/C	Particles	3.4	156.5 at 0.2 C	This work

of the constant current charge and discharge performance test are consistent with those obtained in the rate performance (Fig. 5).

As shown in Fig. 7a, the cyclic voltammetry curves of samples of 675 °C-LFP and 700 °C-LFP were observed, and the redox peak symmetry was high, and the sample curve potential interval of 700 °C was shown. At 0.275 V, the degree of polarization decreases and the reversibility increases, thereby improving conductivity. When the calcination temperature is 650 °C, the redox peak of the synthesized sample is very poor in symmetry compared with the samples of 675 °C and 700 °C, and the width is large, and the peak difference is large because the reaction is still Incomplete, the polarization of the crystal form is not complete and the polarization is severe. When the calcination temperature reached 725 °C (725 °C-LFP) and 750 °C (750 °C-LFP), no significant redox peak was observed, and as the calcination temperature increased, The degree of polarization is gradually increased, and the conductivity is lowered again. This is because the temperature increases and the agglomeration increases, which hinders the diffusion of lithium ions and reduces the electrochemical performance of the material. As shown in Fig. 7b, the AC impedance curves of lithium iron phosphate at different calcination temperatures, The ohmic resistances at different calcination temperatures are 2 Ω cm^{-2}(650 °C-LFP), 6.029 Ω cm^{-2}(675 °C-LFP), 2.129 Ω cm^{-2}(700 °C-LFP), 4.677 Ω cm^{-2}(725 °C-LFP) and 1.764 Ω cm^{-2}(750 °C-LFP).The curve in the high frequency region is semicircular, and the diameter of the semicircle represents the transfer impedance of the charge. The larger the radius, the larger the transfer impedance of the charge and the worse the conductivity. In the low frequency region, the θ angle is the largest at 650 °C-LFP, the diffusion resistance is small, and the conductivity is the best, while the 700 °C-LFP also exhibits good electrical conductivity.

As shown in Fig. 8, the calcination temperature is a cycle performance of a lithium iron phosphate cathode material obtained at different calcination temperatures at 1 C. As can be seen from Fig. 8, the number of cycles is 250, and the discharge specific capacity of 700 °C-LFP is higher than that of other materials. The specific discharge capacity of the second cycle was 124.5 mAh g^{-1}, and the specific discharge capacity at the 250th cycle was 120.7 mAh g^{-1}, and the discharge specific capacity retention rate was 96.9%. When the calcination temperature is 750 °C, the specific discharge capacity is below 43.3 mAh g^{-1}, and the SEM image (Fig. 3) at different calcination temperatures shows that the calcination temperature is 750 °C. When temperature is too high, the excessive temperature causes the excessive growth of crystal grains and the aggregation of material particles, which leads to the increase of the particle size of
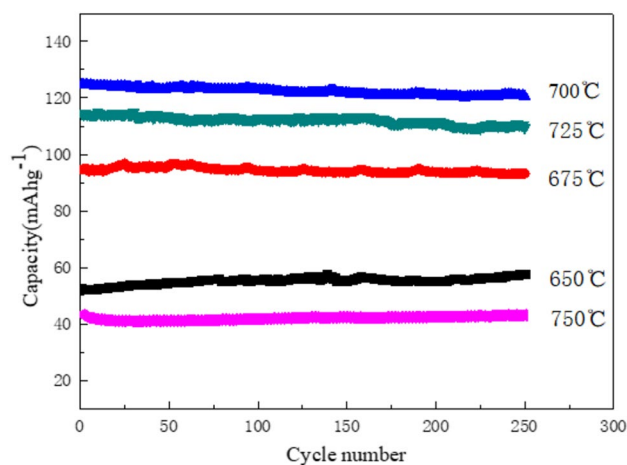
Fig. 8 Sample cycle performance curves of samples at 1 C rate at different calcination temperatures

Fig. 7 Cyclic voltammogram and AC impedance plot of samples at different calcination temperatures
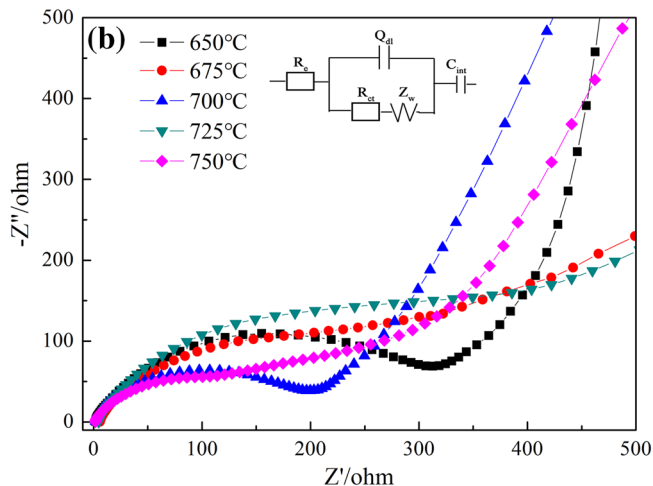
the material, increases the migration distance of lithium ions in the charge and discharge process, and hinders the diffusion of lithium ions, resulting in poor material properties.

4 Conclusions

In short, we have successfully developed a lithium iron phosphate cathode material with better electrochemical performance by sol–gel method. By changing the calcination temperature of $LiFePO_4$/C precursor, cathode materials with different grain size and properties were obtained. It was observed by SEM and EDS that when the lithium iron phosphate carbon containing composite material is calcined at a temperature of 700 °C for 12 h under nitrogen atmosphere, the carbon layer is uniformly coated on the surface of the crystal grains, and the particle size is small (about 80–120 nm), the distribution is relatively uniform, the specific surface area is large, which reduces the migration path of lithium ion in the charge–discharge process, thus improving the utilization rate of active material. The material not only has good conductivity, but also is conducive to the insertion and removal of lithium ions. The first discharge specific capacity at a charging current of 0.2 C was 156.5 mAh g^{-1}. The first discharge specific capacity was 124.5 mAh g^{-1} at a charging current of 1 C. After 250 cycles, the specific discharge capacity was 120.7 mAh g^{-1}, the capacity retention rate was 96.9%, and the electrochemical performance was excellent. The increase in performance stems from structural optimization and may be a promising cathode material for lithium ion batteries for commercial use.

References

1. Z. Sun, H. Cao, X. Zhang et al., Spent lead-acid battery recycling in China—a review and sustainable analyses on mass flow of lead. Waste Manag. **64**, 190–201 (2017)
2. B. Hariprakash, A.K. Shukla, S. Venugoplan, Secondary batteries—nickel systems | nickel–metal hydride: overview. Encycl. Electrochem. Power Sources (2009). https://doi.org/10.1016/B978-044452745-5.00158-1
3. T.K. Ying, X.P. Gao, W.K. Hu et al., Studies on rechargeable NiMH batteries. Int. J. Hydrogen Energy **31**(4), 525–530 (2006)
4. N. Fujioka, A. Taniguchi, et al., Development of nickel/metal-hydride batteries for EVs and HEVs. J. Power Sources **100**(1), 117–124 (2001)
5. L. Cheng, Physical problems involved in lithium ion batteries. Physical **27**(6), 354–357 (1998) (in Chinese)
6. S. Bai, S. Mao, S. Zhu et al., Improved rate and cycling performances of electrodes based on BiFeO3 nanoflakes by compositing with organic pectin for advanced rechargeable Na-Ion batteries. ACS Appl. Nano Mater. **1**(3), 1291–1299 (2018)
7. D. Xu, P. Wang, B. Shen, Synthesis and characterization of sulfur-doped carbon decorated LiFePO4 nanocomposite as high performance cathode material for lithium-ion batteries. Ceram. Int. **42**(4), 5331–5338 (2015)
8. P.P. Prosini, M. Carewska, S. Scaccia et al., Long-term cyclability of nanostructured LiFePO4. Electrochim. Acta **48**(28), 4205–4211 (2003)
9. J. Qian, M. Zhou, Y. Cao et al., Template-free hydrothermal synthesis of nanoembossed mesoporous LiFePO4 microspheres for high-performance lithium-ion batteries. J.Phys.Chem.C **114**(8), 3477–3482 (2011)
10. F. Yu, J. Zhang, Y. Yang et al., Porous micro-spherical aggregates of $LiFePO_4$/C nanocomposites: a novel and simple template-free concept and synthesis via sol–gel-spray drying method. J. Power Sources **195**(19), 6873–6878 (2010)
11. X. Lou, Y. Zhang, Synthesis of $LiFePO_4$/C cathode materials with both high-rate capability and high tap density for lithium-ion batteries. J. Mater. Chem. **21**(12), 4156 (2011)
12. A. Yamada, M. Hosoya, S.C. Chung et al., Olivine-type cathodes: achievements and problems. J. Power Sources **119**(6), 232–238 (2003)
13. S.Y. Chung, J.T. Bloking, Y.M. Chiang, Electronically conductive phosphor-olivines as lithium storage electrodes. Nat. Mater. **1**(2), 123–128 (2002)
14. A. Yamada, S.C. Chung, Crystal chemistry of the olivine-type Li(MnyFe1 − y)PO4and (MnyFe1 − y)PO4 as possible 4V cathode materials for lithium batteries. J. Electrochem. Soc. **148**(8), A960–A967 (2001)
15. K.S. Park, J.T. Son, H.T. Chung et al., Surface modification by silver coating for improving electrochemical properties of LiFePO 4. J. Shangqiu Vocat. Tech. Col. **129**(5), 311–314 (2008)
16. R. Dominko, M. Bele, M. Gaberscek et al., Porous olivine composites synthesized by sol–gel technique. J. Power Sources **153**(2), 274–280 (2006)
17. X. Dong, P. Wang, B. Shen, Synthesis and characterization of sulfur-doped carbon decorated LiFePO 4 nanocomposite as high performance cathode material for lithium-ion batteries. Ceram. Int. **42**(4), 5331–5338 (2016)
18. H. Huang, S.C. Yin, L.F. Nazar, Approaching theoretical capacity of LiFePO4 at room temperature at high rates. Electrochem. Solid-State Lett. **4**(10), A170–A172 (2001)
19. S. Tobishima, M. Takahashi, et al. Reaction behavior of LiFePO4 as a cathode material for rechargeable lithium batteries. Solid State Ionics Diffus. React. **148**(3), 283–289 (2002)
20. H. Liu, Z. Wang, X. Li et al., Synthesis and electrochemical properties of olivine LiFePO4prepared by a carbothermal reduction method. J. Power Sources **184**(2), 469–472 (2008)
21. Q. Gu, X. Gu, W. Gao, Research progress of lithium iron phosphate used as cathode materia. Anhui Chem. Ind. **37**(4), 13–15 (2011) (in Chinese)
22. K. Naoi, K. Kisu, E. Iwama et al., Ultrafast charge-discharge characteristics of a nanosized core-shell structured LiFePO\r, 4\r, material for hybrid supercapacitor applications. Energy Environ. Sci. **9**(6), 2143–2151 (2016)
23. K.F. Hsu, S.Y. Tsay, B.J. Hwang, Synthesis and characterization of nano-sized LiFePO4 cathode materials prepared by a citric acid-based sol–gel route. J. Mater. Chem. **14**(17), 2690–2695 (2004)
24. C. Wang Fuqing, Wu Jian, Minghao, Y. Baolian, Propylene oxide-assisted fast sol–gel synthesis of mesoporous and nano-structured LiFePO4/C cathode materials. Ionics **19**(3), 451–460 (2013)
25. H.P. Liu, Z.X. Wang, X.H. Li et al., synthesis and electrochemical properties of olivine LiFePO4 prepared by a carbothermal reduction method. J. Power Sources, **184**(2), 469–472 (2008)
26. L.B. Kong, P. Zhang, M.C. Liu et al., Fabrication of promising LiFePO4/C composite with a core–shell structure by amoderate

in situ carbothermal reduction method. Electrochim. Acta **70**, 19–24 (2012)

27. I. Rahayu, S. Hidayat, L. Aryadi, Synthesis of LiFePO4/Pani/C composite as a cathode material for lithium ion battery. AIP Conf. Proc. **1712**(1), (2016)

28. K. Naoi, K. Kisu, E. Iwama et al., Ultrafast charge–discharge characteristics of a nanosized core–shell structured LiFePO4 material for hybrid supercapacitor applications. Energy Environ. Sci. **9**(6), 2143–2151 (2016)

29. J.K. Kim, J.W. Choi, G.S. Chauhan et al., Enhancement of electrochemical performance of lithium iron phosphate by controlled sol-gel synthesis. Electrochim. Acta **53**(28), 8258–8264 (2008)

30. R. Dominko, J.M. Goupil, M. Bele et al., Impact of LiFePO4/C composites porosity on their electrochemical performance. J. Electrochem. Soc. **152**(5), 858–863 (2005)

31. R. Dominko, M. Bele, M. Gaberscek et al., Impact of the carbon coating thickness on the electrochemical performance of LiFePO4/C composites. J. Electrochem. Soc. **152**(3), 607–610 (2005)

32. G. Qin, Q. Ma, C. Wang, A porous C/LiFePO 4 /multiwalled carbon nanotubes cathode material for Lithium ion batteries. Electrochim. Acta **115**(3), 407–415 (2014)